IETE Technical Review

ISSN: (Print) (Online) Journal homepage: https://www.tandfonline.com/loi/titr20

Performance of a Method for the Estimation of Carrier and Sampling Frequency Offsets in OFDM WLAN Systems

Qi Cheng

To cite this article: Qi Cheng (2023) Performance of a Method for the Estimation of Carrier and Sampling Frequency Offsets in OFDM WLAN Systems, IETE Technical Review, 40:3, 371-379, DOI: 10.1080/02564602.2022.2118876

To link to this article: https://doi.org/10.1080/02564602.2022.2118876

Published online: 11 Sep 2022.

IETE TECHNICAL REVIEW
2023, VOL. 40, NO. 3, 371–379
https://doi.org/10.1080/02564602.2022.2118876

RESEARCH ARTICLE

OPEN ACCESS

Performance of a Method for the Estimation of Carrier and Sampling Frequency Offsets in OFDM WLAN Systems

Qi Cheng

School of Engineering, Design and Built Environment, Western Sydney University, Locked Bag 1797, Penrith MC, 1797 NSW, Australia

ABSTRACT
A method was published in 2020 for the estimation of the residual carrier frequency offset (RCFO) and sampling frequency offset (SFO) in WLAN OFDM systems. The purpose of this paper is to compare this method with one existing method for more examples to make a fair comparison in terms of estimation accuracy and computational load.

KEYWORDS
OFDM; CFO; Residual CFO; SFO; Weighted Least Squares

1. INTRODUCTION AND MODEL OF DATA SYMBOLS

A method was proposed in [1] for the estimation of the RCFO and SFO. It is compared with the methods in [2, 3] and the maximum-likelihood methods in [4, 5]. In [1], limited simulation results were presented, and one particular concern is that the method in [1] always performs better than the method in [3]. In this paper, more cases are considered to provide a fair comparison between the method in [1] and the method in [3]. Our finding is that the method in [3] can also outperform that in [1] in some cases.

A WLAN OFDM system is considered in this paper. In this system, each data symbol contains $N = 64$ samples and $N_{cp} = 16$ samples of cyclic prefix at the beginning. The cyclic prefix is the replica of the 16 samples at the end. It is used to combat multipath channel impact and is dropped at the receiver. Sixty-four subcarriers are allocated to each user. Among those subcarriers, only $P = 56$ subcarriers are active. Fifty-two active subcarriers are used to transmit (unknown) information-bearing symbols. The remaining four subcarriers are reserved to transmit (known) pilot symbols. All subcarriers are represented by indices: $-32, \ldots, -1, 0, 1, \ldots, 31$. The active subcarrier indices are given in the set

$$\mathcal{K} = [-28, \ldots, -1, 1, \ldots, 28], \tag{1}$$

and the indices of the four pilot subcarriers are given in the set

$$\mathcal{P} \stackrel{def}{=} [p_1, p_2, p_3, p_4] = [-21, -7, 7, 21]. \tag{2}$$

Subcarriers with indices $-32, \ldots, -29, 29, \ldots, 31$ form the guard band on the two sides of the spectrum.

Information-bearing symbols are randomly taken from the QPSK constellation for each data symbol and then fixed. Pilot symbols are randomly chosen from the BPSK constellation and are fixed for all data symbols. Note that pilot symbols are allowed to vary in a known pattern in IEEE 802.11a standards [6], but in this paper, we consider the simple case of the same pilot symbols for all data symbols.

Denote the RCFO by ϵ. The RCFO is obtained by subtracting a course estimate of a fractional CFO from it [7]. The fractional CFO is within the subcarrier spacing, and the RCFO is even much smaller. Denote the SFO by ζ. IEEE 802.11a standards [6] recommend that the accuracy of the oscillator sampling frequency be within the range ± 100 ppm, that is equivalent to

$$|\zeta| \leq 10^{-4}. \tag{3}$$

An L-tap multipath channel is defined by complex coefficients h_l, $l = 0, 1, \ldots, L-1$. The channel frequency response at the subcarrier frequency with index k is defined as

$$H_k = \sum_{l=0}^{L-1} h_l z_0^{-k}. \tag{4}$$

The sampling instant of the first sample in the cyclic prefix of the first data symbol is chosen as the start of time. Then the last N samples of the received data of ith data symbol with the impact of the CFO/channel can be

represented as

$$y_i(n) = z_0^{\epsilon(1+\zeta)(n_i+n)} \sum_{k\in\mathcal{K}} z_0^{k\zeta(n_{0,i}+n)+kn} H_k s_i(k),$$
$$z_0 = e^{j2\pi/N}, \quad n = 0, 1, \ldots, N-1,\ i = 1, 2, \ldots, I \tag{5}$$

where I is the total number of data symbols collected at the receiver, $n_{0,i} = (N + N_{cp})(i-1)$, $n_i = n_{0,i} + N_{cp}$ and $s_i(k)$, $\forall k \in \mathcal{K}$ contain information-bearing (unknown) symbols and pilot (known) symbols of the ith (OFDM) data symbol. H_k in (5) is assumed to remain constant during the collection of I data symbols. But it varies among different simulation runs.

In practice, received data symbols are corrupted by noise. The noisy received ith data symbol is written as

$$\hat{y}_i(n) = y_i(n) + \xi_i(n) \tag{6}$$

where $\xi_i(n)$ are measurement noise quantities of the ith data symbol. $\xi_i(n)$ are assumed to be Gaussian with i.i.d. (independent and identically distributed) real and imaginary parts of mean zero and variance $\sigma^2/2$. The noise is also assumed to be independent of the channel.

The problem of this paper is to determine ϵ, ζ from noisy data symbols in (6).

2. REVIEW OF EXISTING METHODS

The methods in [1–3] will be reviewed in this section.

Demodulated samples of the ith compensated data symbol at the pilot subcarriers are equal to its DFT and are given by

$$\begin{aligned} Y_i(p_m) &= (1/N) \sum_{n=0}^{N-1} y_i(n) z_0^{-p_m n} \\ &= z_0^{N_{cp}\epsilon} z_0^{(\epsilon+\zeta p_m)n_{0,i}} H_{p_m} s_i(p_m) \\ &\quad + z_0^{\epsilon N_{cp}} \sum_{k\in\mathcal{K}} z_0^{(\epsilon+\zeta k)n_{0,i}} H_k s_i(k) \\ &\quad \cdot \left(\sum_{n=0}^{N-1} (z_0^{(\epsilon+\zeta k)n} - 1) z_0^{(k-p_m)n} / N \right) \qquad (7) \\ &\approx z_0^{N_{cp}\epsilon} z_0^{(\epsilon+\zeta p_m)n_i} H_{p_m} s_i(p_m), \quad p_m \in \mathcal{P} \qquad (8) \end{aligned}$$

where the approximation is based on the assumption that the RCFO and SFO are *sufficiently* small. For details, readers can refer to (20) and Figure 1 in [7].

The methods in [1–3] are based on the correlation of any two adjacent data symbols. The correlation for the ith and $(i+1)$st data symbols is defined as

$$r_i(p_m) = (Y_i(p_m))^* Y_{i+1}(p_m), \quad p_m \in \mathcal{P}. \tag{9}$$

From (8), one can have

$$r_i(p_m) \approx |H_{p_m}|^2 |s_i(p_m)|^2 z_0^{(\epsilon+p_m\zeta)(N+N_{cp})}, \quad p_m \in \mathcal{P} \tag{10}$$

where $s_i(p_m) = s_{i+1}(p_m)$ is used. Multiple correlations at a pilot subcarrier are combined and written as

$$r(p_m) = \sum_{i=1}^{I-1} r_i(p_m), \quad p_m \in \mathcal{P}. \tag{11}$$

From (10) and the assumption of sufficiently small ϵ and ζ, estimates of ϵ and ζ are found from the following equation for m = 1,2,3,4:

$$\epsilon + p_m\zeta = \left[\angle r(p_m)\right] / (2\pi((N+N_{cp})/N)), \quad p_m \in \mathcal{P} \tag{12}$$

where $\angle$ denotes the phase of a complex number.

Define

$$\hat{Y}_i(p_m) = (1/N) \sum_{n=0}^{N-1} \hat{y}_i(n) z_0^{-p_m n} \tag{13}$$

$$\hat{r}(p_m) = \sum_{i=1}^{I-1} (\hat{Y}_i(p_m))^* \hat{Y}_{i+1}(p_m), \quad p_m \in \mathcal{P}. \tag{14}$$

Let

$$\hat{\phi}(p_m) = \left[\angle \hat{r}(p_m)\right] / (2\pi((N+N_{cp})/N)) \tag{15}$$

$$\hat{\boldsymbol{\phi}} = [\hat{\phi}(p_1), \hat{\phi}(p_2), \hat{\phi}(p_3), \hat{\phi}(p_4)]^T \tag{16}$$

$$\mathbf{a}_1 = \begin{bmatrix} 1 \\ 1 \\ 1 \\ 1 \end{bmatrix}, \quad \mathbf{a}_2 = \begin{bmatrix} p_1 \\ p_2 \\ p_3 \\ p_4 \end{bmatrix} \tag{17}$$

$$\mathbf{A} = [\mathbf{a}_1 \quad \mathbf{a}_2]. \tag{18}$$

Then it is well known that a weighted least-squares (WLS) method for joint estimation of ϵ and ζ can be given as [3]

$$\begin{bmatrix} \hat{\epsilon}_{wls} \\ \hat{\zeta}_{wls} \end{bmatrix} = (\mathbf{A}^T\mathbf{Q}\mathbf{A})^{-1}\mathbf{A}^T\mathbf{Q}\hat{\boldsymbol{\phi}} \tag{19}$$

where $\mathbf{Q}$ is a positive-definite real matrix ($\mathbf{Q}^T = \mathbf{Q}$).

Define the following noise-free phase vector:

$$\boldsymbol{\phi} = \mathbf{A}\begin{bmatrix}\epsilon\\ \zeta\end{bmatrix}. \tag{20}$$

Then the phase estimation covariance matrix can be written as

$$E\{(\hat{\boldsymbol{\phi}} - \boldsymbol{\phi})(\hat{\boldsymbol{\phi}} - \boldsymbol{\phi})^T\} \stackrel{def}{=} (\mathbf{Q}_0)^{-1} \tag{21}$$

where the statistical expectation E in (21) is taken with respect to noise quantities for non-random RCFO, SFO and a non-random channel. For random channels, though one can still define such a covariance matrix, an explicit expression is extremely difficult to obtain. It is proven in [3] that when $\mathbf{Q} = \mathbf{Q}_0$ in (19), the WLS method yields estimates of the smallest covariances. That method will be called the optimum WLS (OWLS) method. It was proposed in [3]. The OWLS estimates of ϵ and ζ from (19) are given by

$$\begin{bmatrix}\hat{\epsilon}_{owls}\\ \hat{\zeta}_{owls}\end{bmatrix} = (\mathbf{A}^T\mathbf{Q}_0\mathbf{A})^{-1}\mathbf{A}^T\mathbf{Q}_0\hat{\boldsymbol{\phi}}. \tag{22}$$

In WLAN systems, the pilot subcarrier indices satisfy the property that $p_1 = -p_4, p_2 = -p_3$. Hence, $\mathbf{a}_1^T\mathbf{a}_2 = 0$, and, when $\mathbf{Q}$ in (19) becomes an identity matrix, the matrix in inversion becomes a diagonal one and the WLS method reduces to the least-squares (LS) method (without weighting) in [2]. The LS method yields estimates of ϵ and ζ given by

$$\begin{aligned}\begin{bmatrix}\hat{\epsilon}_{ls}\\ \hat{\zeta}_{ls}\end{bmatrix} &= \begin{bmatrix}(\mathbf{a}_1^T\mathbf{a}_1)^{-1} & 0\\ 0 & (\mathbf{a}_2^T\mathbf{a}_2)^{-1}\end{bmatrix}\begin{bmatrix}\mathbf{a}_1^T\hat{\boldsymbol{\phi}}\\ \mathbf{a}_2^T\hat{\boldsymbol{\phi}}\end{bmatrix}\\ &= \begin{bmatrix}(\mathbf{a}_1^T\mathbf{a}_1)^{-1}\mathbf{a}_1^T\hat{\boldsymbol{\phi}}\\ (\mathbf{a}_2^T\mathbf{a}_2)^{-1}\mathbf{a}_2^T\hat{\boldsymbol{\phi}}\end{bmatrix}.\end{aligned} \tag{23}$$

The method in [1] is called successive interference (SIC) cancellation-based weighted least-squares estimation. Hereafter, it will be called the SIC method. Based on the relationships (10) and (12), the SIC estimates of ϵ and ζ are given by [1]

$$\hat{\epsilon}_{sic} = \left[\angle\left(\sum_{m=1}^{4}\hat{r}_{p_m}\right)\right]/(2\pi((N+N_{cp})/N)) \tag{24}$$

$$\hat{\zeta}_{sic} = (\mathbf{a}_2^T\mathbf{Q}_0\mathbf{a}_2)^{-1}\mathbf{a}_2^T\mathbf{Q}_0(\hat{\boldsymbol{\phi}} - \mathbf{a}_1\hat{\epsilon}_{sic}). \tag{25}$$

The SIC method differs from the OWLS method in the estimation of the RCFO. In (24), correlations of the four pilot subcarriers are added first, and a single phase is obtained next. In contrast, in the OWLS method, four phases are obtained from the correlations for all pilot subcarriers. In this paper, the main purpose is to investigate whether the calculation of a single phase for the RCFO can always lead to accuracy improvement. In the numerical comparison section, it will be demonstrated that this is not always true.

According to the analysis (performed for two data symbols and but also applicable to multiple data symbols) in [3], at high signal-to-noise ratio and for non-random sufficiently small RCFO/SFO and for a non-random channel, $\mathbf{Q}_0$ is approximately a diagonal matrix and its diagonal elements can be written as $\alpha|H_{p_m}|^2$ for $p_m \in \mathcal{P}$ as given in (33) of [3]. Here, $|\cdot|$ denotes the magnitude of a complex number. Note that α contains the contribution of other unknown quantities, but remains unchanged $\forall m$. Thus one can drop α and replace those diagonal elements with $|H_{p_m}|^2$ without affecting the performances of the OWLS and SIC methods. In practice, the noiseless channel frequency response $|H_{p_m}|^2$ is not available. Based on (8), it is substituted by its estimate

$$|\hat{H}_{p_m}|^2 = \sum_{i=1}^{I}|\hat{Y}_i(p_m)|^2/I. \tag{26}$$

Note: In [1], the LS method and OWLS method were incorrectly referenced to [21] and [20] of that paper. Those two papers were published in IEICE journals in 2019, but they are not the original contributors of the LS and OWLS methods.

3. ESTIMATION ERROR EXPRESSION

To verify simulation results, a first-order approximation is adopted to derive first-order estimation error expressions in this section. The symbol $\doteq$ is used to denote the first order approximation. In the first order approximation, only constant terms and first-order terms of ϵ, ζ and noise quantities are kept.

Let

$$\begin{aligned}b_{i,p_m} &= z_0^{\epsilon N_{cp}}\sum_{k\in\mathcal{K}} z_0^{(\epsilon+\zeta k)n_{0,i}}H_k s_i(k)\\ &\quad\cdot\left(\sum_{n=0}^{N-1}(z_0^{(\epsilon+\zeta k)n} - 1)z_0^{(k-p_m)n}/N\right).\end{aligned} \tag{27}$$

Then according to (13), the noisy demodulated samples can be rewritten as

$$\begin{aligned}\hat{Y}_i(p_m) &= (1/N)\sum_{n=0}^{N-1}\hat{y}_i(n)z_0^{-p_m n}\\ &= z_0^{\epsilon N_{cp}}z_0^{(\epsilon+\zeta p_m)n_{0,i}}H_{p_m}s_i(p_m) + b_{i,p_m}\end{aligned}$$

$$+ (1/N)\sum_{n=0}^{N-1}\xi_i(n)z_0^{-p_m n}$$
$$= z_0^{\epsilon N_{cp}} z_0^{(\epsilon+\zeta p_m)n_{0,i}} H_{p_m} s_i(p_m) + b_{i,p_m} + (1/N)\sum_{n=0}^{N-1}\xi_i(n)z_0^{-p_m n}. \quad (28)$$

Also let

$$c_{i,p_m} = b_{i,p_m} + (1/N)\sum_{n=0}^{N-1}\xi_i(n)z_0^{-p_m n}. \quad (29)$$

Then one can obtain

$$\hat{Y}_i(p_m) \doteq z_0^{\epsilon N_{cp}} z_0^{(\epsilon+\zeta p_m)n_{0,i}} H_{p_m} s_i(p_m) + c_{i,p_m}. \quad (30)$$

Finally, the correlation of the noisy demodulated samples in the two adjacent data symbols at a pilot subcarrier can be written as

$$\begin{aligned}
&(\hat{Y}_i(p_m))^* \hat{Y}_{i+1}(p_m) \\
&= z_0^{(\epsilon+\zeta p_m)(N+N_{cp})}|H_{p_m}|^2|s_i(p_m)|^2 \\
&\quad + z_0^{-\epsilon N_{cp}} z_0^{-(\epsilon+\zeta p_m)n_{0,i}}(H_{p_m}s_i(p_m))^* c_{i+1,p_m} \\
&\quad + c_{i,p_m}^* z_0^{\epsilon N_{cp}} z_0^{(\epsilon+\zeta p_m)n_{0,i+1}} H_{p_m} s_{i+1}(p_m) \\
&\quad + c_{i,p_m}^* c_{i+1,p_m} \\
&\doteq [1 + j(2\pi(N+N_{cp})/N)(\epsilon+\zeta p_m)] \\
&\quad \times |H_{p_m}|^2|s_i(p_m)|^2 \\
&\quad + z_0^{-\epsilon N_{cp}} z_0^{-(\epsilon+\zeta p_m)n_{0,i}}(H_{p_m}s_i(p_m))^* c_{i+1,p_m} \\
&\quad + c_{i,p_m}^* z_0^{\epsilon N_{cp}} z_0^{(\epsilon+\zeta p_m)n_{0,i+1}} H_{p_m} s_{i+1}(p_m) \\
&\stackrel{def}{=} [1 + j(2\pi(N+N_{cp})/N)(\epsilon+\zeta p_m)] \\
&\quad \times |H_{p_m}|^2|s_i(p_m)|^2 \\
&\quad + d_{i,p_m}^*(H_{p_m}s_i(p_m))^* c_{i+1,p_m} \\
&\quad + c_{i,p_m}^* d_{i+1,p_m}(H_{p_m}s_{i+1}(p_m)).
\end{aligned}$$

Then the sum of all correlations is given by

$$\begin{aligned}
\hat{r}(p_m) &= \sum_{i=1}^{I-1}(\hat{Y}_i(p_m))^*\hat{Y}_{i+1}(p_m) \\
&\doteq [1 + j(2\pi(N+N_{cp})/N)(\epsilon+\zeta p_m)] \\
&\quad \cdot \sum_{i=1}^{I-1}|H_{p_m}|^2|s_i(p_m)|^2 \\
&\quad + j\Im\left(\sum_{i=1}^{I-1} d_{i,p_m}^*(H_{p_m}s_i(p_m))^* c_{i+1,p_m}\right) \\
&\quad + j\Im\left(\sum_{i=1}^{I-1} c_{i,p_m}^* d_{i+1,p_m}(H_{p_m}s_{i+1}(p_m))\right)
\end{aligned}$$

where $\Im$ denotes the imaginary part of a complex number. Since $s_i(p_m) = s_1(p_m)$ for $i \in [2,\ldots,I]$ and they are BPSK symbols, then

$$\begin{aligned}
\sum_{i=1}^{I-1}|H_{p_m}|^2|s_i(p_m)|^2 &= (I-1)|H_{p_m}|^2|s_1(p_m)|^2 \\
&= (I-1)|H_{p_m}|^2.
\end{aligned}$$

Hence

$$\begin{aligned}
&\frac{\hat{r}(p_m)}{(I-1)|H_{p_m}|^2} \\
&\doteq 1 + j(2\pi(N+N_{cp})/N)(\epsilon+\zeta p_m) \\
&\quad + j\Im\left(\frac{\sum_{i=1}^{I-1} d_{i,p_m}^*(H_{p_m}s_i(p_m))^* c_{i+1,p_m}}{(I-1)|H_{p_m}|^2}\right) \\
&\quad + j\Im\left(\frac{\sum_{i=1}^{I-1} c_{i,p_m}^* d_{i+1,p_m}(H_{p_m}s_{i+1}(p_m))}{(I-1)|H_{p_m}|^2}\right) \\
&\stackrel{def}{=} 1 + j(2\pi(N+N_{cp})/N)(\epsilon+\zeta p_m + f_{p_m})
\end{aligned}$$

and the estimated phases are equal to

$$\begin{aligned}
\angle\hat{r}(p_m) &= \angle\frac{\hat{r}(p_m)}{(I-1)|H_{p_m}|^2} \\
&\doteq (2\pi(N+N_{cp})/N)(\epsilon+\zeta p_m + f_{p_m}). \quad (31)
\end{aligned}$$

Define $\mathbf{f} = [f_{p_1}, f_{p_2}, f_{p_3}, f_{p_4}]^T$. Then the OWLS estimation errors are given by

$$\begin{aligned}
\begin{bmatrix}\hat{\epsilon}_{owls} - \epsilon \\ \hat{\zeta}_{owls} - \zeta\end{bmatrix} &= (\mathbf{A}^T\mathbf{Q}_0\mathbf{A})^{-1}\mathbf{A}^T\mathbf{Q}_0(\hat{\boldsymbol{\phi}} - \boldsymbol{\phi}) \\
&= (\mathbf{A}^T\mathbf{Q}_0\mathbf{A})^{-1}\mathbf{A}^T\mathbf{Q}_0\mathbf{f}. \quad (32)
\end{aligned}$$

From

$$\begin{aligned}
\sum_{m=1}^{4}\hat{r}(p_m) &\doteq 1 + j(2\pi(N+N_{cp})/N)(I-1)\epsilon\sum_{m=1}^{4}|H_{p_m}|^2 \\
&\quad + j(2\pi(N+N_{cp})/N)(I-1)\zeta\sum_{m=1}^{4}p_m|H_{p_m}|^2 \\
&\quad + j\sum_{m=1}^{4}\Im\left(\sum_{i=1}^{I-1} d_{i,p_m}^*(H_{p_m}s_i(p_m))^* c_{i+1,p_m}\right)
\end{aligned}$$

$$+ j \sum_{m=1}^{4} \Im \left(\sum_{i=1}^{I-1} c^*_{i,p_m} d_{i+1,p_m} (H_{p_m} s_{i+1}(p_m)) \right),$$

one obtains that

$$\begin{aligned}
\angle \sum_{m=1}^{4} \hat{r}(p_m) \doteq\ & (2\pi(N+N_{cp})/N)(I-1)\epsilon \sum_{m=1}^{4} |H_{p_m}|^2 \\
& + (2\pi(N+N_{cp})/N) \\
& \times (I-1)\zeta \sum_{m=1}^{4} p_m |H_{p_m}|^2 \\
& + \sum_{m=1}^{4} \Im \left(\sum_{i=1}^{I-1} d^*_{i,p_m} (H_{p_m} s_i(p_m))^* c_{i+1,p_m} \right) \\
& + \sum_{m=1}^{4} \Im \left(\sum_{i=1}^{I-1} c^*_{i,p_m} d_{i+1,p_m} (H_{p_m} s_{i+1}(p_m)) \right).
\end{aligned}$$

Then the SIC RCFO estimate is equal to

$$\begin{aligned}
\hat{\epsilon}_{sic} &= \frac{\angle \sum_{m=1}^{4} \hat{r}(p_m)}{(2\pi(N+N_{cp})/N)(I-1)\sum_{m=1}^{4} |H_{p_m}|^2} \\
&\doteq \epsilon + \frac{\zeta \sum_{m=1}^{4} p_m |H_{p_m}|^2}{\sum_{m=1}^{4} |H_{p_m}|^2} \\
&\quad + \frac{\sum_{m=1}^{4} \Im \left(\sum_{i=1}^{I-1} d^*_{i,p_m} (H_{p_m} s_i(p_m))^* c_{i+1,p_m} \right)}{(2\pi(N+N_{cp})/N)(I-1)\sum_{m=1}^{4} |H_{p_m}|^2} \\
&\quad + \frac{\sum_{m=1}^{4} \Im \left(\sum_{i=1}^{I-1} c^*_{i,p_m} d_{i+1,p_m} (H_{p_m} s_{i+1}(p_m)) \right)}{(2\pi(N+N_{cp})/N)(I-1)\sum_{m=1}^{4} |H_{p_m}|^2} \\
&\stackrel{def}{=} \epsilon + c_{eps}
\end{aligned}$$

and the corresponding estimation error is given by

$$\hat{\epsilon}_{sic} - \epsilon = c_{eps}. \tag{33}$$

Next, the SIC SFO estimate can be shown to be equal to

$$\begin{aligned}
\hat{\zeta}_{sic} - \zeta &= (\mathbf{a}_2^T \mathbf{Q}_0 \mathbf{a}_2)^{-1} \mathbf{a}_2^T \mathbf{Q}_0 ((\hat{\boldsymbol{\phi}} - \boldsymbol{\phi}) - \mathbf{a}_1 (\hat{\epsilon}_{sic} - \epsilon)) \\
&= (\mathbf{a}_2^T \mathbf{Q}_0 \mathbf{a}_2)^{-1} \mathbf{a}_2^T \mathbf{Q}_0 (\mathbf{f} - \mathbf{a}_1 c_{eps}).
\end{aligned} \tag{34}$$

4. COMPUTATION LOAD ANALYSIS

In [1], no details were given on how the computational loads are calculated for the OWLS and SIC methods. In this section, a detailed analysis is provided. For analysis convenience, only the first two data symbols are considered in 4.1 adn 4.2. The result obtained there can be easily extended to the case of more data symbols in 4.3.

In the implementation of the OWLS and SIC methods, each diagonal element of $\mathbf{Q}_0$ in (21) is replaced by $|\hat{H}_{p_m}|^2$ and can be calculated using 2 real multiplications and 1 real addition from $\hat{Y}_i(p_m)$ in (7). Thus $\mathbf{Q}_0$ can be computed using 8 real multiplications and 4 real additions. In this section, a division is counted as (equivalent to) 1 multiplication and a subtraction is counted as 1 addition.

$\hat{r}(p_m), \forall p_m \in \mathcal{P}$ have to be calculated from the demodulated samples, using 4 complex multiplications for 2 data symbols. Next, $\hat{\phi}(p_m)$, $\forall p_m \in \mathcal{P}$ are calculated from $\hat{r}(p_m)$, $\forall p_m \in \mathcal{P}$. In this step, the tangent values have to be calculated from 4 real divisions followed by the inverse tangent operations. To simplify analysis, a tangent (inverse tangent) operation is counted as 1 multiplication. This requires 8 real multiplications. These two steps are required by both the OWLS and SIC methods.

4.1 OWLS Method

By exploiting the symmetry of the pilot locations, $\mathbf{A}^T\mathbf{Q}_0\mathbf{A}$ can be written as

$$\begin{bmatrix} \sum_{m=3}^{4} a_m & \sum_{m=3}^{4} p_m b_m \\ \sum_{m=3}^{4} p_m b_m & \sum_{m=3}^{4} (p_m)^2 a_m \end{bmatrix}$$

where $a_m = |\hat{H}_{p_m}|^2 + |\hat{H}_{p_{5-m}}|^2$ and $b_m = |\hat{H}_{p_m}|^2 - |\hat{H}_{p_{5-m}}|^2$. Values of $(p_m)^2, m = 3, 4$ can be precalculated and stored. The squared channel frequency responses are added/subtracted first, and then multiplied with pilot indices or their squares. After those multiplications, additions are still required. Hence, from $\mathbf{Q}_0$, one can calculate $\mathbf{A}^T\mathbf{Q}_0\mathbf{A}$ using 4 real multiplications and $4+6=10$ real additions.

From $\mathbf{A}^T\mathbf{Q}_0\mathbf{A}$, one can calculate $(\mathbf{A}^T\mathbf{Q}_0\mathbf{A})^{-1}$ using 6 real multiplications and 1 real additions.

Due to the symmetry of the pilot locations, $\mathbf{A}^T\mathbf{Q}_0\hat{\boldsymbol{\phi}}$ can also be written as

$$\begin{bmatrix} \sum_{m=3}^{4} (|\hat{H}_{p_m}|^2 \hat{\phi}(p_m) + |\hat{H}_{p_{5-m}}|^2 \hat{\phi}(p_{5-m})) \\ \sum_{m=3}^{4} p_m (|\hat{H}_{p_m}|^2 \hat{\phi}(p_m) - |\hat{H}_{p_{5-m}}|^2 \hat{\phi}(p_{5-m})) \end{bmatrix}.$$

Hence, from $\mathbf{Q}_0$, one can calculate $\mathbf{A}^T\mathbf{Q}_0\hat{\boldsymbol{\phi}}$ using $4+2=6$ real multiplications and $2+2=4$ real additions.

As analyzed in the second last paragraph of 6.2 of [7], from $\mathbf{A}^T\mathbf{Q}_0\mathbf{A}$ and $\mathbf{A}^T\mathbf{Q}_0\hat{\boldsymbol{\phi}}$, $(\mathbf{A}^T\mathbf{Q}_0\mathbf{A})^{-1}\cdot\mathbf{A}^T\mathbf{Q}_0\hat{\boldsymbol{\phi}}$ requires 7 real multiplications and 3 real additions.

The computational load of the OWLS method is summarized in Table 1, where additions are omitted.

4.2 SIC Method

The RCFO estimation $\mathbf{a}_1^T\hat{\mathbf{r}}$ requires 4 complex additions.

Note that $\mathbf{a}_2^T\mathbf{Q}_0\mathbf{a}_2 = \sum_{m=3}^{4}(p_m)^2(|\hat{H}_{p_m}|^2 + |\hat{H}_{p_{5-m}}|^2)$. This requires 2 real multiplications and 4 real additions.

$\mathbf{a}_2^T\mathbf{Q}_0\hat{\boldsymbol{\phi}} = \sum_{m=3}^{4} p_m(|\hat{H}_{p_m}|^2\hat{\phi}(p_m) - |\hat{H}_{p_{5-m}}|^2\hat{\phi}(p_{5-m}))$. This requires 6 real multiplications and 4 real additions.

$(\mathbf{a}_2^T\mathbf{Q}_0\mathbf{a}_2)^{-1}\cdot\mathbf{a}_2^T\mathbf{Q}_0\hat{\boldsymbol{\phi}}$ requires further 1 real division (equivalent to one multiplication).

The computational load of the SIC method is summarized in Table 2, where additions are omitted.

4.3 Comparison

One complex multiplication is equivalent to 4 real multiplications. In terms of the number of complex multiplications, the OWLS computational load is 13.75 and the SIC computational load is 10.5.

The RCFO and SFO estimations are followed by compensation, to remove the impact of these two frequency offsets, to recover information-bearing symbols. The computational load of an estimation method should include the load of compensation. The computational load of the demodulated samples in (13) is not counted because it is an inherent part of an OFDM receiver.

Compensation is performed by multiplying $z_0^{-(\hat{\epsilon}+\hat{\zeta}k)n_i}$ $\forall k \in \mathcal{K}$ to the demodulated samples of each data symbol. Here, $\hat{\epsilon}$ and $\hat{\zeta}$ are the RCFO and SFO estimates. Those demodulated samples have the same form as $Y_i(p_m)$ in (7) if p_m is replaced by k. The calculation of $z_0^{-(\hat{\epsilon}+\hat{\zeta}k)n_i}$ $\forall k \in \mathcal{K}$ requires at least P complex multiplications. Multiplying these factors to all samples requires additional P complex multiplications. For I data symbols, the SIC computational load is $\mathcal{L}_{sic} = 10.5(I-1) + 4PI$, and the OWLS load is $\mathcal{L}_{owls} = 13.75(I-1) + 4PI$. For $I = 2$, one obtains that $\mathcal{L}_{owls}/\mathcal{L}_{sic} = 1.0071$, $\mathcal{L}_{owls}/\mathcal{L}_{sic} = 1.0125$ for $I = 10$, $\mathcal{L}_{owls}/\mathcal{L}_{sic} = 1.0132$ for $I = 20$, and $\mathcal{L}_{owls}/\mathcal{L}_{sic} = 1.0135$ for $I = 40$. Hence, in this case, the saving provided by the SIC method is no more than 1.4%.

Table 1: Numbers of multiplications in individual steps required by the OWLS method (two data-symbol case)

	Complex multiplication	Real multiplication
$\mathbf{Q}_0$		8
$\hat{r}(p_m),\ \forall p_m \in \mathcal{P}$	4	
$\hat{\boldsymbol{\phi}}$		8
$\mathbf{A}^T\mathbf{Q}_0\mathbf{A}$		4
$(\mathbf{A}^T\mathbf{Q}_0\mathbf{A})^{-1}$		6
$\mathbf{A}^T\mathbf{Q}_0\hat{\boldsymbol{\phi}}$		6
$(\mathbf{A}^T\mathbf{Q}_0\mathbf{A})^{-1}$ $\cdot\mathbf{A}^T\mathbf{Q}_0\hat{\boldsymbol{\phi}}$		7
Total	4	39

Table 2: Numbers of multiplications in individual steps required by the SIC method (two data-symbol case)

	Complex multiplication	Real multiplication
$\mathbf{Q}_0$		8
$\hat{r}(p_m),\ \forall p_m \in \mathcal{P}$	4	
$\sum_{m=1}^{4}\hat{r}(p_m)$		1
$\hat{\boldsymbol{\phi}}$		8
$\mathbf{a}_2^T\mathbf{Q}_0\mathbf{a}_2$		2
$\mathbf{a}_2^T\mathbf{Q}_0\hat{\boldsymbol{\phi}}$		6
$(\mathbf{a}_2^T\mathbf{Q}_0\mathbf{a}_2)^{-1}$ $\cdot\mathbf{a}_2^T\mathbf{Q}_0\hat{\boldsymbol{\phi}}$		1
Total	4	26

5. NUMERICAL COMPARISON

In this section, numerical evaluations will be used to compare the OWLS and SIC methods in terms of the estimation accuracy.

The parameters $\epsilon = 10^{-2}$ and $\zeta = 10^{-4}$ were fixed in all simulation runs. Rayleigh channels were used and varying for various simulation runs. Each Rayleigh channel has $L = 12$ taps with power delay profiles of $E\{|h_l|^2\} = e^{-l/12}$, $l = 0, 1, \ldots, L-1$. The signal-to-noise ratio is defined as SNR $= 10\log_{10}[P/(N\sigma^2)]$ (dB).

The estimation accuracy is measured by the root-mean squared error (RMSE) of estimates produced by a method in multiple runs of Monte Carlo simulation. The RCFO RMSE is defined as

$$\sqrt{\sum_{i=1}^{N_{sim}}(\hat{\epsilon}^i - \epsilon)^2/N_{sim}}$$

where $\hat{\epsilon}^i$ is an estimate of ϵ given by a method in the ith simulation run and $N_{sim} = 2000$ is the total number of

simulation runs. The SFO RMSE is defined as

$$\sqrt{\sum_{i=1}^{N_{sim}} (\hat{\zeta}^i - \zeta)^2 / N_{sim}}$$

where $\hat{\zeta}^i$ is an estimate of ζ generated along with $\hat{\epsilon}^i$ by the same method in the ith simulation run. Simulated RMSEs will be denoted by the notation "simu". Calculated RMSEs using (32), (33), (34), will be denoted by the notation "cal".

The performance of the LS method was always the poorest in all simulation examples, and thus its RMSEs will not be shown.

First, the SIC and OWLS are compared for $I = 2$ versus SNR which is the same case as in Figures 1–2 of

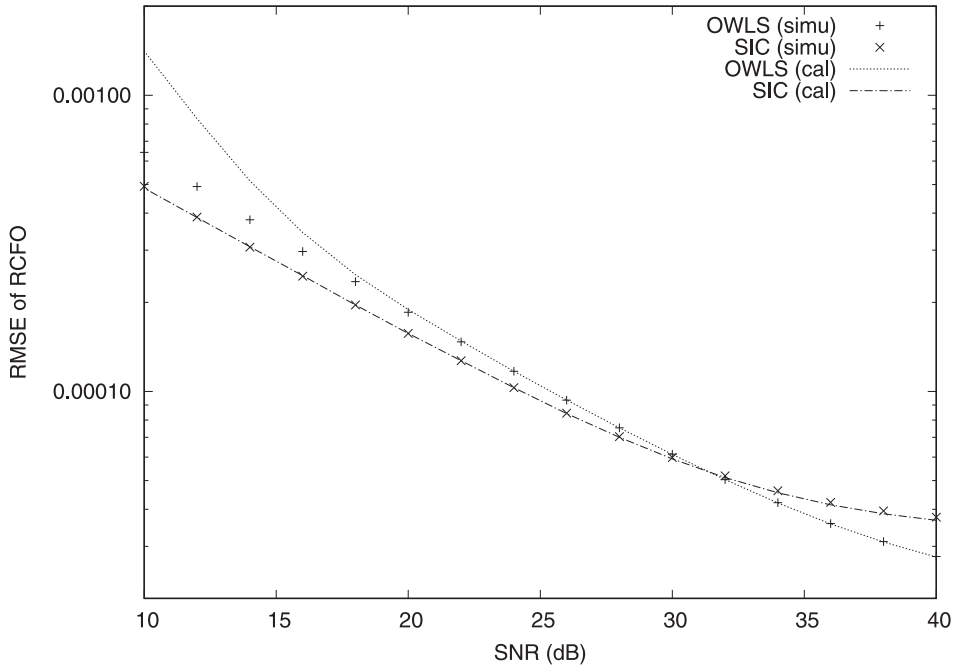

Figure 1: RMSEs of ϵ, versus SNR, for the SIC and OWLS methods. The number of data symbols is $I = 2$

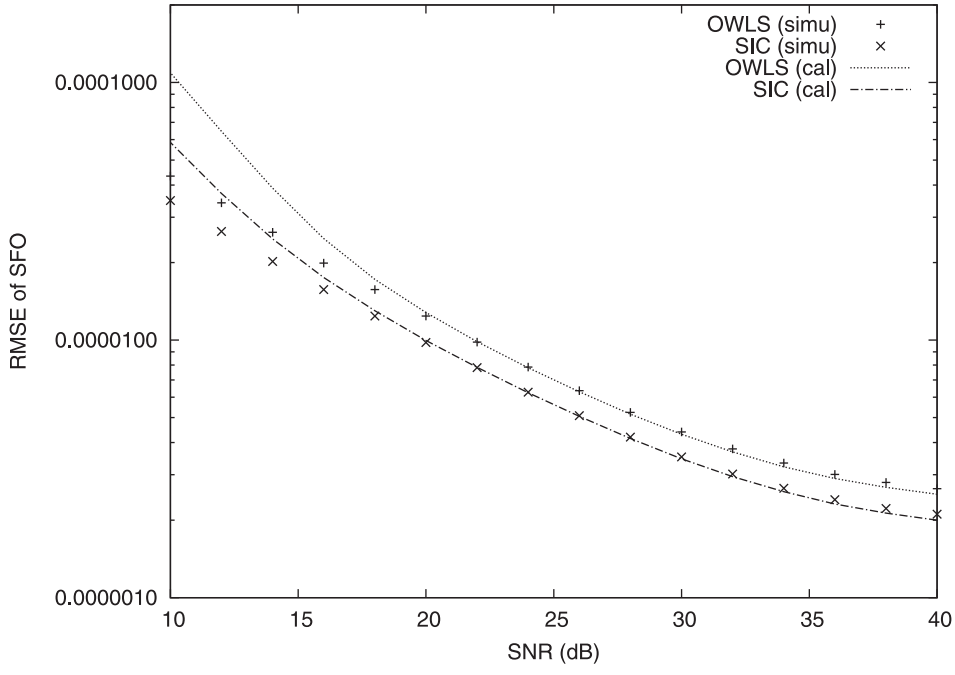

Figure 2: RMSEs of ζ, versus SNR, for the SIC and OWLS methods. The number of data symbols is $I = 2$

[1]. The RMSEs of ϵ are shown in Figure 1. The RMSEs of ζ are shown in Figure 2. Calculated RMSEs are very close to simulated RMSEs for high SNRs. When SNR is below 18 dB, calculated RMSEs do not match simulated RMSEs because the estimation error is not small enough and the first-order perturbation is no longer valid. *In this example, the SIC method performs better than the OWLS method (except for the RCFO at the high SNR range).*

Next, the SIC and OWLS methods are compared for SNR $=$ 20 dB and SNR $=$ 26 dB versus I, the number of data symbols. The RMSEs of ϵ are shown in Figure 3. The

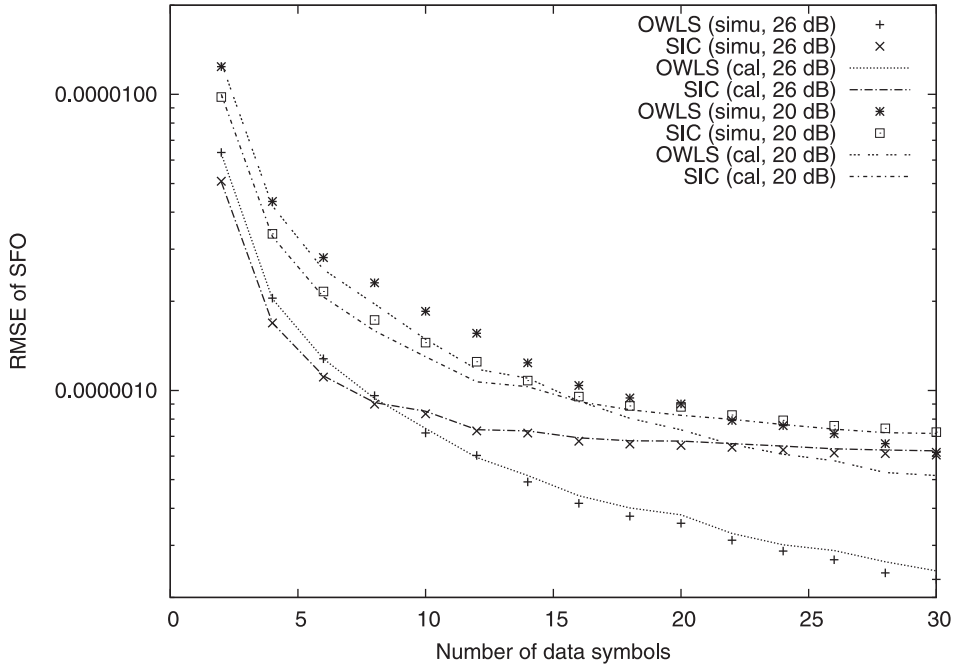

Figure 3: RMSEs of ϵ, versus the number of data symbols (I), for the SIC and OWLS methods. SNR $=$ 20 dB and SNR $=$ 26 dB

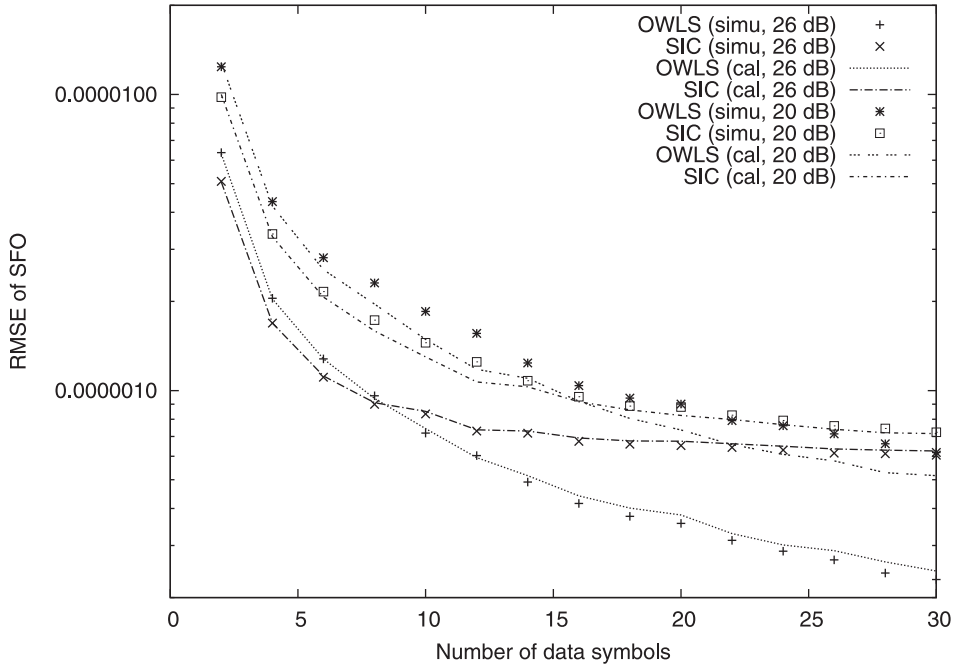

Figure 4: RMSEs of ζ, versus the number of data symbols (I), for the SIC and OWLS methods. SNR $=$ 20 dB and SNR $=$ 26 dB

RMSEs of ζ are shown in Figure 4. Calculated RMSEs are very close to simulated RMSEs for SNR = 26 dB. But this is not the case for SNR = 20 dB, probably due to not very small errors. *However, in this example, the SIC method performs worse than the OWLS method when the number of data symbols is large.*

6. CONCLUSION

The SIC method is compared with the OWLS method. For a small number of data symbols, the SIC method provides more accurate RCFO and SFO estimates. However, for a large number of data symbols, the OWLS method provides more accurate RCFO and SFO estimates.

The RCFO and SFO estimations are always followed by compensation for the retrieval of information-bearing symbols. Based on our analysis, compensation constitutes the most computational load for both methods; and as a result, the computational advantage offered by the SIC method is marginal.

DISCLOSURE STATEMENT

No potential conflict of interest was reported by the author.

REFERENCES

1. X. Zhou, K. Zheng, B. Wu and H. Zhao, "Successive interference cancellation-based weighted least-squares estimation of carrier and sampling frequency offsets for WLANs," *IEEE Access*, Vol. 8, pp. 210678–84, Oct 2020.
2. M. Sliskovic, "Carrier and sampling frequency offset estimation and correction in multicarrier systems," in *Proceedings of the GLOBALCOM*, Vol. 1, San Antonio, TX, Nov. 2001, pp. 285–9.
3. P. Tsai, H. Kang and T. Chieuh, "Joint weighted least-squares estimation of carrier-frequency offset and timing offset for OFDM systems over multipath fading channels," *IEEE Trans. Veh. Technol.*, Vol. 54, no. 1, pp. 211–23, Jan. 2005. DOI:10.1109/TVT.2004.838891
4. X. Wang and B. Hu, "A low-complexity ML estimator for carrier and sampling frequency offsets in OFDM systems," *IEEE Commun. Lett.*, Vol. 18, no. 3, pp. 503–6, 2014. DOI:10.1109/LCOMM.2013.123113.132444
5. Y. Kim and J. Lee, "Joint maximum likelihood estimation of carrier and sampling frequency offsets for OFDM systems," *IEEE Trans. Broadcast.*, Vol. 57, no. 2, pp. 277–83, 2011. DOI:10.1109/TBC.2011.2122890
6. IEEE Std 802.11ac – 2013 *IEEE Standard for Information Technology – Telecommunications and information exchange between systems – Local and metropolitan area networks – Specific requirements – Part 11: Wireless LAN Medium Access Control (MAC) and Physical Layer (PHY) Specifications – Amendment 4: Enhancements for Very High Throughput for Operation in Bands below 6 GHz.*
7. Q. Cheng, "Joint estimation of carrier and sampling frequency offsets using OFDM WLAN preamble," *Wireless Pers. Commun.*, Vol. 98, no. 2, pp. 2121–61, Jan. 2018. DOI:10.1007/s11277-017-4967-8

Author

Qi Cheng obtained the Bachelor's of Engineering degree from Anhui University, China, in 1982, the Master of Engineering degree from the Institute of Electronics of the Chinese Academia in 1985, and the PhD degree from the University of Melbourne, Australia, in 1995. He has been a research fellow at the University of Melbourne and taught a wide range of subjects in computer, electrical and telecommunication engineering, and assumed various academic administrative roles, at the Northern Territory University and Western Sydney University. He is currently a lecturer at the Western Sydney University. Cheng has published more than 40 technical papers in international conferences and journals. He is also a co-editor of the book '*High Resolution Signal Processing*' (Editors: Y. Hua, A. Gershman, Q. Cheng) published by Marcel Dekker in 2003. He has been TPC members and session chairs for various international conferences.

Corresponding author. Email: q.cheng@westernsydney.edu.au